Towards understanding the detection of profile asymmetry from Mueller matrix differential decomposition

Xiuguo Chen,[1] Hao Jiang,[1,a)] Chuanwei Zhang,[1,2] and Shiyuan Liu[1,2,a)]
[1]*State Key Laboratory of Digital Manufacturing Equipment and Technology, Huazhong University of Science and Technology, Wuhan 430074, China*
[2]*Wuhan Eoptics Technology Co. Ltd., Wuhan 430075, China*

(Received 10 September 2015; accepted 29 November 2015; published online 14 December 2015)

The Mueller matrix differential decomposition is applied to interpret Mueller matrices of asymmetric gratings and to understand the use of Mueller matrix ellipsometry (MME) in distinguishing the direction of profile asymmetry, as reported in our recent work [Chen *et al.*, J. Appl. Phys. **116**, 194305 (2014)]. We show that both linear and circular birefringence-dichroism pairs can be extracted from the collected Mueller matrices, which provide a complete description of the sample polarization properties. We present both theoretical and experimental results, which demonstrate that the linear birefringence and dichroism, LB′ and LD′, along the ±45° axes are the origin of the MME in distinguishing the direction of profile asymmetry. We also demonstrate that equal magnitude of profile asymmetry in opposite directions always yields LB′ and LD′ of the same absolute deviation from zero and of opposite sign, when the plane of incidence is no longer perpendicular to grating lines. The sensitivity of LB′ and LD′ to both the magnitude and direction of profile asymmetry is useful in monitoring processes in which symmetric structures are desired. © *2015 AIP Publishing LLC*.
[http://dx.doi.org/10.1063/1.4937558]

I. INTRODUCTION

Due to the rich information provided by the 4×4 Mueller matrices, such as anisotropy and depolarization, Mueller matrix ellipsometry (MME), also known as Mueller matrix polarimetry, has demonstrated a great potential in the nondestructive characterization of geometrical parameters of nanostructures, such as critical dimension, sidewall angle, and feature height.[1] Recent studies further revealed that conventional spectroscopic ellipsometry (SE) has difficulties in measuring asymmetric gratings due to the lack of capability of distinguishing the direction of profile asymmetry. Elements of the two 2×2 off-diagonal blocks of the Mueller matrix exhibit good sensitivity to both the magnitude and direction of profile asymmetry at a conical mounting with the plane of incidence parallel to grating lines.[2–4] Despite the unique capability of MME for the unambiguous detection of asymmetric gratings, the underlying origin behind the use of MME in distinguishing the direction of profile asymmetry has not been fully explored yet, to the best of our knowledge.

In this work, we apply the differential decomposition to investigate Mueller matrices of asymmetric gratings. Although 16 elements of a Mueller matrix contain all the information about the light-matter interaction that one can extract from the linear polarization scattering, it is generally impossible to relate individual Mueller matrix elements to the elementary optical properties of a sample, because all the optical properties are lumped into the collected Mueller matrices. The differential Mueller matrix calculus[5] provides a powerful technique for determining the optical properties of anisotropic media. A differential decomposition approach[6,7] was proposed to obtain the 4×4 differential Mueller matrix by taking the logarithm of the collected Mueller matrix. From the differential Mueller matrix, the sample elementary optical properties can be directly obtained, including the linear birefringence along the *p*-*s* and ±45° axes, the linear dichroism along the *p*-*s* and ±45° axes, and the circular birefringence and dichroism, which provide a complete description of the sample polarization properties. We find and demonstrate that, among these elementary properties, the linear birefringence and dichroism along the ±45° axes exhibit sensitivity to both the magnitude and direction of asymmetric profiles at any conical mounting (with the plane of incidence no longer perpendicular to grating lines), while other elementary properties at most show sensitivity to the magnitude of profile asymmetry. The significance of our finding is that the linear birefringence and dichroism along the ±45° axes will be a useful and robust metric for monitoring processes in which symmetric structures are desired.

II. THEORY

In MME-based nanostructure metrology, the specular (zeroth-) order diffracted light is by far the most commonly measured order. It is because that the specular order usually has a large intensity and hence the measurement provides a good signal-to-noise ratio. In addition, the specular order is also the only order that always exists. The Jones matrix **J** associated with the specular diffraction order of a grating sample, which connects the incident Jones vector with the reflected one, can be formulated by

$$\begin{bmatrix} E_{rp} \\ E_{rs} \end{bmatrix} = \mathbf{J} \begin{bmatrix} E_{ip} \\ E_{is} \end{bmatrix} = \begin{bmatrix} r_{pp} & r_{ps} \\ r_{sp} & r_{ss} \end{bmatrix} \begin{bmatrix} E_{ip} \\ E_{is} \end{bmatrix}, \quad (1)$$

a)Authors to whom correspondence should be addressed. Electronic mails: hjiang@hust.edu.cn (H. Jiang) and shyliu@hust.edu.cn (S. Liu).

where $E_{s,p}$ refers to the electric field components that are perpendicular and parallel to the plane of incidence, respectively. The Jones matrix $\mathbf{J}$ can be written as[8]

$$\mathbf{J} = e^{-i\chi}\begin{bmatrix} \cos\frac{T}{2} - \frac{iL}{T}\sin\frac{T}{2} & \frac{(C - iL')}{T}\sin\frac{T}{2} \\ -\frac{(C + iL')}{T}\sin\frac{T}{2} & \cos\frac{T}{2} + \frac{iL}{T}\sin\frac{T}{2} \end{bmatrix}, \quad (2)$$

in which $i = \sqrt{-1}$, $\chi = \eta - i\kappa$, $L = LB - iLD$, $L' = LB' - iLD'$, $C = CB - iCD$, and $T = \sqrt{L^2 + L'^2 + C^2}$. η and κ refer to the isotropic phase retardation and amplitude absorption, LB and LD refer to the linear birefringence and dichroism along the *p-s* axes of the reference frame, LB′ and LD′ refer to the linear birefringence and dichroism along the ±45° axes (with respect to the *p-s* axes), CB and CD refer to the circular birefringence and dichroism. In the absence of depolarization, the Mueller matrix $\mathbf{M}$ can be calculated directly from the Jones matrix $\mathbf{J}$ by

$$\mathbf{M} = \begin{bmatrix} m_{11} & m_{12} & m_{13} & m_{14} \\ m_{21} & m_{22} & m_{23} & m_{24} \\ m_{31} & m_{32} & m_{33} & m_{34} \\ m_{41} & m_{42} & m_{43} & m_{44} \end{bmatrix} = \mathbf{U}(\mathbf{J} \otimes \mathbf{J}^*)\mathbf{U}^{-1}, \quad (3a)$$

where m_{ij} is the (i, j)th Mueller matrix element, the symbol $\otimes$ denotes the Kronecker product, $\mathbf{J}^*$ is the complex conjugate of $\mathbf{J}$, and the matrix $\mathbf{U}$ is given by

$$\mathbf{U} = \begin{bmatrix} 1 & 0 & 0 & 1 \\ 1 & 0 & 0 & -1 \\ 0 & 1 & 1 & 0 \\ 0 & i & -i & 0 \end{bmatrix}. \quad (3b)$$

The Mueller matrix $\mathbf{M}$ calculated from Eq. (3) is also called a nondepolarizing Mueller matrix or a Mueller-Jones matrix.

In the differential Mueller matrix calculus, the differential Mueller matrix $\mathbf{m}$ relates the Mueller matrix $\mathbf{M}$ to its spatial derivative along the light propagation direction z as[5]

$$d\mathbf{M}/dz = \mathbf{mM}. \quad (4)$$

If the differential Mueller matrix $\mathbf{m}$ does not depend on z, the solution of Eq. (4) can be achieved by taking the logarithm of $\mathbf{M}$,[6,7] that is,

$$\mathbf{L} = \ln(\mathbf{M}) = \mathbf{L}_m + \mathbf{L}_u, \quad (5a)$$

$$\mathbf{L}_m = \frac{1}{2}(\mathbf{L} - \mathbf{GL}^T\mathbf{G}) = \begin{bmatrix} 0 & -LD & -LD' & CD \\ -LD & 0 & CB & LB' \\ -LD' & -CB & 0 & -LB \\ CD & -LB' & LB & 0 \end{bmatrix}, \quad (5b)$$

$$\mathbf{L}_u = \frac{1}{2}(\mathbf{L} + \mathbf{GL}^T\mathbf{G}) = \begin{bmatrix} A & \Delta p_1 & \Delta p_2 & \Delta p_3 \\ -\Delta p_1 & A - A_1 & \Delta p_4 & \Delta p_5 \\ -\Delta p_2 & \Delta p_4 & A - A_2 & \Delta p_6 \\ -\Delta p_3 & \Delta p_5 & \Delta p_6 & A - A_3 \end{bmatrix}, \quad (5c)$$

where $\mathbf{L}$ is the accumulated differential Mueller matrix: $\mathbf{L} = l\mathbf{m}$, with l being the optical path length in the medium, and the superscript "T" denotes the matrix transpose; $\mathbf{G}$ is the Minkowski metric, and $\mathbf{G} = \mathrm{diag}(1, -1, -1, -1)$; A is the isotropic absorption, A_i $(i = 1, 2, 3)$ denote the anisotropic absorption (or depolarization) along the *p-s*, ±45°, and circular axes, respectively; Δp_i $(i = 1, 2, \ldots, 6)$ stand for the uncertainties of the six elementary properties (LD, LD′, CD, CB, LB′, and LB, respectively) resulting from depolarization. According to Eq. (5), we know that the G-antisymmetric term $\mathbf{L}_m$ (namely, $\mathbf{GL}_m^T\mathbf{G} = -\mathbf{L}_m$) and G-symmetric term $\mathbf{L}_u$ (namely, $\mathbf{GL}_u^T\mathbf{G} = \mathbf{L}_u$) of $\mathbf{L}$ contain the mean values and uncertainties of the elementary properties, respectively, together with the anisotropic absorption, of a sample Mueller matrix $\mathbf{M}$. If $\mathbf{M}$ is a nondepolarizing Mueller matrix, we always have $\mathbf{L}_u = 0$ within the experimental (or numerical) error, provided that A$\mathbf{I}$ has been subtracted beforehand from $\mathbf{L}$ ($\mathbf{I}$ is an identity matrix). The Mueller matrix differential decomposition given in Eq. (5) has a straightforward application in transmission measurements. Although we can also obtain the accumulated differential Mueller matrix $\mathbf{L}$ by implementing the differential decomposition to the measured Mueller matrix in reflection, here $\mathbf{L}$ will not be a direct read of the elementary phenomenological optical properties of the sample as it happens in transmission. The calculation of the accumulated differential Mueller matrix $\mathbf{L}$ by Eq. (5) in reflection, as will be seen in the remainder of this paper, should be understood as a pure mathematical operation used to reveal the minimum number of independent parameters that are necessary to describe the polarization change upon reflection.

According to the principle of electromagnetic reciprocity, when a light beam passes through the media (or is reflected or scattered) in the reverse direction, the corresponding reciprocal Jones matrix $\hat{\mathbf{J}}$ and reciprocal Mueller matrix $\hat{\mathbf{M}}$ can be represented by[9]

$$\hat{\mathbf{J}} = \mathbf{TJ}^T\mathbf{T}^{-1}, \quad (6a)$$

$$\hat{\mathbf{M}} = \mathbf{OM}^T\mathbf{O}^{-1}, \quad (6b)$$

respectively, where the matrices $\mathbf{T} = \mathrm{diag}(1, -1)$ and $\mathbf{O} = \mathrm{diag}(1, 1, -1, 1)$ account for the change in the coordinate system due to the reversal of motion. $\mathbf{T}^{-1}$ and $\mathbf{O}^{-1}$ are the inverses of $\mathbf{T}$ and $\mathbf{O}$, respectively. Without loss of generality, assuming that the wavelength and incident angle are fixed λ and θ, respectively, we denote $\mathbf{M}(\Delta\alpha, \phi)$ as the Mueller matrix of an asymmetric grating with a sidewall tilt of $\Delta\alpha$ ($\Delta\alpha = \alpha_1 - \alpha_2 \neq 0$), as depicted in Fig. 1, and obtained at the azimuthal angle of ϕ, and $\mathbf{M}(\Delta\alpha, \phi + \pi)$ as the Mueller matrix obtained after a rotation of the sample by π around the z axis. According to Eq. (6), we have

$$\mathbf{M}(\Delta\alpha, \phi + \pi) = \mathbf{OM}(\Delta\alpha, \phi)^T\mathbf{O}^{-1}. \quad (7)$$

Since the rotation of the sample by π around the z axis is equivalent to the change of the sidewall tilting direction, Eq. (7) is thereby also equivalent to

$$\mathbf{M}(-\Delta\alpha, \phi) = \mathbf{OM}(\Delta\alpha, \phi)^T\mathbf{O}^{-1}. \quad (8)$$

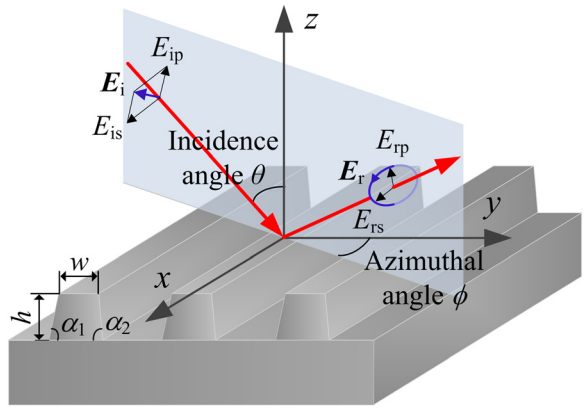

FIG. 1. Representation of polarized light incidence upon a one-dimensional grating structure with sidewall tilting.

From Eq. (8), we can further derive that

$$\mathbf{L}_m(-\Delta\alpha,\ \phi) = \mathbf{O}\mathbf{L}_m(\Delta\alpha,\ \phi)^T\mathbf{O}^{-1}, \tag{9}$$

where $\mathbf{L}_m(\Delta\alpha,\ \phi)$ is the G-antisymmetric term of $\ln[\mathbf{M}(\Delta\alpha,\ \phi)]$. According to Eqs. 5(b) and (9), we have

$$\mathrm{L}(-\Delta\alpha,\ \phi) = \mathrm{L}(\Delta\alpha,\ \phi), \tag{10a}$$

$$\mathrm{L}'(-\Delta\alpha,\ \phi) = -\mathrm{L}'(\Delta\alpha,\ \phi), \tag{10b}$$

$$\mathrm{C}(-\Delta\alpha,\ \phi) = \mathrm{C}(\Delta\alpha,\ \phi). \tag{10c}$$

Equation (10) indicates that the origin of MME in distinguishing the direction of profile asymmetry is the linear birefringence and dichroism, LB′ and LD′, along the ±45° axes. In comparison, other elementary optical properties (LB, LD, CB, and CD) at most show sensitivity to the magnitude of profile asymmetry.

III. RESULTS AND DISCUSSION

A. Simulation results

To give an intuitive understanding of the Mueller matrix detection of profile asymmetry, we simulated the Mueller matrix spectra of a one-dimensional Si grating structure with the sidewall tilting shown in Fig. 1 at different azimuthal angles using rigorous coupled-wave analysis.[10] In the simulation, the Si grating has a period of 800 nm, a top critical dimension of $w = 350$ nm, a line height of $h = 470$ nm, and takes $\alpha_1 = 88°$, $\alpha_2 = 82°$ for a left sidewall tilt ($\Delta\alpha = 5°$), and $\alpha_1 = 82°$, $\alpha_2 = 88°$ for a right sidewall tilt ($\Delta\alpha = -5°$), and $\alpha_1 = \alpha_2 = 85°$ for a symmetric profile ($\Delta\alpha = 0°$). The optical constants of Si are taken from the literature.[11] The wavelength λ is varied from 200 to 800 nm with increments of 5 nm. The incidence angle θ is fixed at 65°, and the azimuthal angle ϕ is varied from 0° to 90° with increments of 30°. Figure 2 depicts the difference spectra $\Delta m_{ij}(\Delta\alpha)$ between Mueller matrices calculated for the investigated grating structure with asymmetric ($\Delta\alpha = \pm 5°$) and symmetric ($\Delta\alpha = 0°$) profiles, namely, $\Delta m_{ij}(\Delta\alpha) = m_{ij}(\Delta\alpha) - m_{ij}(\Delta\alpha = 0°)$ ($i, j = 1, 2, 3, 4$). We chose four typical elements m_{12}, m_{13}, m_{14}, and m_{33} from the 4×4 Mueller matrix (normalized to m_{11}), of which m_{12} and m_{33} are, respectively, equal to $\alpha = -\cos 2\Psi$ and $\beta = \sin 2\Psi \cos\Delta$ in conventional SE (Ψ and Δ are the ellipsometric angles),[12,13] and m_{13} and m_{14} are elements from the upper right 2×2 off-diagonal block of the Mueller matrix. As shown in Fig. 2, when $\phi = 0°$, i.e., with the plane of incidence perpendicular to grating lines, m_{12} and m_{33} are insensitive to the direction of profile asymmetry, which indicates that conventional SE is incapable of distinguishing the left and right sidewall tilts. When $\phi = 0°$, m_{13} and m_{14} are insensitive to both the magnitude and direction of profile asymmetry. However, when $\phi \neq 0°$, especially when $\phi = 90°$, m_{13} and m_{14} exhibit noticeable sensitivity to both the magnitude and direction of profile asymmetry and in the latter case we observe that

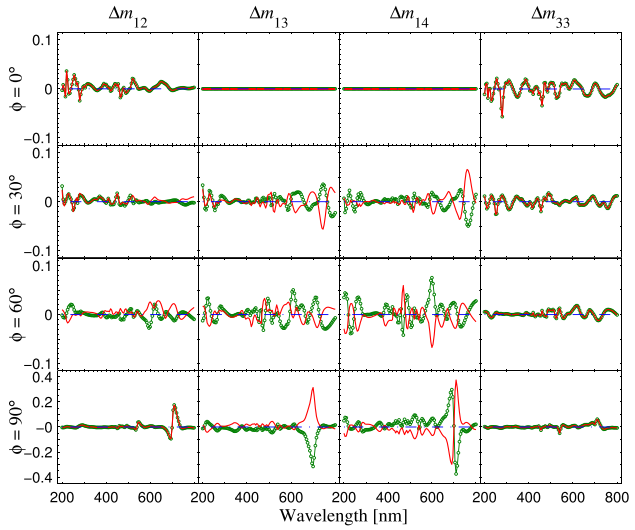

FIG. 2. The difference spectra of Mueller matrix elements m_{12}, m_{13}, m_{14}, and m_{33} between that calculated for the investigated grating structure with asymmetric and symmetric profiles at different azimuthal angles. The green solid curves with open circles and the red solid curves correspond to asymmetric profiles with left and right sidewall tilts, respectively.

$$\Delta m_{13}(\Delta\alpha) = -\Delta m_{13}(-\Delta\alpha), \tag{11a}$$

$$\Delta m_{14}(\Delta\alpha) = -\Delta m_{14}(-\Delta\alpha). \tag{11b}$$

We then performed differential decomposition to the simulated Mueller matrices. Because the simulated Mueller matrices do not contain depolarization, the G-symmetric term will be $\mathbf{L}_u = 0$ within the numerical error. The six elementary optical properties LB, LD, LB′, LD′, CB, and CD of the investigated grating structure at different azimuthal angles can be obtained according to Eq. (5). As can be observed from Fig. 3, LB and LD, as well as CB and CD, are indeed insensitive to the direction of profile asymmetry at any azimuthal angle. Compared with other elementary properties, LB′ and LD′ exhibit noticeable sensitivity to both the magnitude and direction of profile asymmetry at any azimuthal configuration except $\phi = 0°$. Moreover, when the plane of incidence is no longer perpendicular to grating lines, i.e., $\phi \neq 0°$, equal sidewall tilt in opposite directions always yields LB′ and LD′ of opposite sign, as revealed in Eq. (10b).

The result shown in Fig. 3 can be further interpreted according to the reciprocity theorem for the specular order

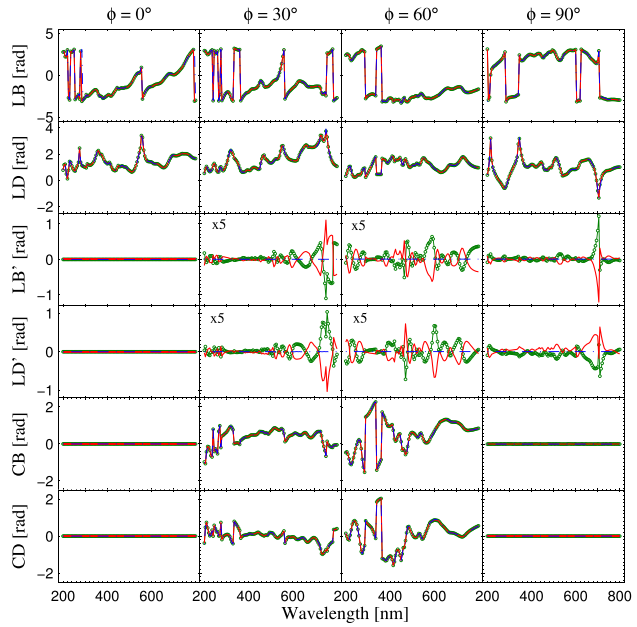

FIG. 3. The spectra of elementary optical properties LB, LD, LB′, LD′, CB, and CD extracted from the simulated Mueller matrices presented in Fig. 2. The green solid curves with open circles and the red solid curves correspond to asymmetric profiles with left and right sidewall tilts, respectively. The blue dashed-dotted curves correspond to the symmetric profile. The LB′ and LD′ obtained at $\phi = 30°$ and $\phi = 60°$ are multiplied by a factor of 5.

diffraction of a multilayer bianisotropic grating,[14] which states that, for any incident light (λ, θ, ϕ) and for the coordinate system defined in Fig. 1, the Jones matrix associated with the specular diffraction order satisfies $\mathbf{J} = \hat{\mathbf{J}}$, provided that (i) the grating is composed of only reciprocal materials, (ii) the constitutive tensors of all grating media possess the C_{2z} symmetry, and (iii) the grating's tomography has the σ_y symmetry. Here, C_{2z} and σ_y are standard symbols in group theory used to denote the symmetry operations and symmetry types.[15] From this reciprocity theorem, we can further derive that $\mathrm{L}' = 0$, i.e., $\mathrm{LB}' = 0$ and $\mathrm{LD}' = 0$, as well as the reciprocal property of the associated Mueller matrix, i.e., $\mathbf{M} = \hat{\mathbf{M}}$, for any azimuthal configuration. The sidewall tilting breaks the σ_y symmetry, which thereby leads to $\mathbf{J} \neq \hat{\mathbf{J}}$, $\mathrm{L}' \neq 0$, and $\mathbf{M} \neq \hat{\mathbf{M}}$.

Among the various azimuthal configurations, two special cases are of great interest. The first case is that when $\phi = 0°$, all diffraction orders are within the plane of incidence and this configuration is usually called planar diffraction. In this case, the relation $\mathbf{J} = \hat{\mathbf{J}}$ is trivially satisfied because the cross-polarization coefficients r_{ps} and r_{sp} are zero for any periodic structure even if it has an asymmetric profile. Hence, the two 2×2 off-diagonal blocks of the Mueller matrix vanish, and the optical properties LB′, LD′, CB, and CD are all equal to zero, as presented in Fig. 3. Another case is a special conical mounting of $\phi = 90°$, where all diffraction orders are on the surface of a cone with revolution symmetry around the direction of grating lines. At this mounting, the relation $\mathbf{J} = \hat{\mathbf{J}}$ is also trivially satisfied for symmetric gratings, because both r_{ps} and r_{sp} are zero. However, when profile symmetry is broken, r_{ps} and r_{sp} will be different from zero. According to Theorem 3 of Ref. 14, we know that $r_{ps} = r_{sp}$, namely, the associated Jones matrix is a symmetric matrix, i.e., $\mathbf{J} = \mathbf{J}^{\mathrm{T}}$, at this special conical mounting. We further know from Eq. (2) that at this mounting $\mathrm{C} = 0$, i.e., $\mathrm{CB} = 0$ and $\mathrm{CD} = 0$, even for asymmetric gratings, as also revealed in Fig. 3. According to Eq. (3), we can derive the relations between elements of off-diagonal blocks of the associated Mueller matrix that $m_{13} = m_{31}$, $m_{23} = m_{32}$, $m_{14} = -m_{41}$, and $m_{24} = -m_{42}$. From Eq. (8), we can further derive the relation that

$$m_{ij}(\Delta\alpha) = -m_{ij}(-\Delta\alpha), \tag{12}$$

for any element of the two 2×2 off-diagonal blocks of the Mueller matrix, which means that equal sidewall tilt in opposite directions also yields Mueller matrix off-diagonal blocks of opposite sign. Equation (11) can therefore be readily derived from Eq. (12). However, we should note that Eq. (12) is not necessarily valid at other general conical mountings ($\phi = 30°$ and $\phi = 60°$), since CB and CD are no longer equal to zero when $\phi \neq 90°$,[16] as indicated in Fig. 3.

As reported in the previous work,[2–4] asymmetric profiles can be discriminated by examining whether the two 2×2 off-diagonal blocks of the collected Mueller matrix at $\phi = 90°$ vanish or not. However, we have to point out that this judgment may be disturbed by the mechanical positioning error (mainly the systematic error) in practice. It is because an offset from $\phi = 90°$ will also lead to nonzero Mueller matrix off-diagonal blocks, even for a symmetric profile. In comparison, LB′ and LD′ are immune to practical mechanical positioning error, which is expected to be a more robust metric in this sense for monitoring processes, where symmetric structures are desired. In addition, although the result presented in Fig. 3 did not take depolarization into account, it is worth pointing out that the achieved conclusions are valid. Even in the presence of depolarization, it can be readily demonstrated by considering that any physical depolarizing Mueller matrix is equivalent to the spatial or temporal averaging of a number of nondepolarizing Mueller matrices[17,18] and the property in Eqs. (7)–(10) is still preserved under linear addition. It is also worth pointing out that the nonzero CB and CD at the general conical mountings presented in Fig. 3 do not necessarily suggest that the grating sample exhibits chirality or bianisotropy. **L** is obtained from Eq. (5) and is defined in a transmission setup, and the values obtained in a reflection setup are not a direct read of the true elementary optical properties of the sample. Anyway, we should note that Eqs. (6)–(10) are still valid even in a reflection setup, which thereby guarantees the validity of the achieved conclusions.

B. Experimental results

We have also conducted an experimental demonstration of the above-achieved conclusions. In the experiment, a set of STU220 resist films with a thickness of ~240 nm (developed by Obducat AB Co.) were spin-coated onto Si wafers. Soft UV nanoimprint lithography was then performed on an Eitre3 Nano Imprinter using a Si imprinting mold. The Si mold, whose scanning electron microscopy (SEM) (Nova NanoSEM450, FEI Co.) image is shown in Fig. 4(a), was

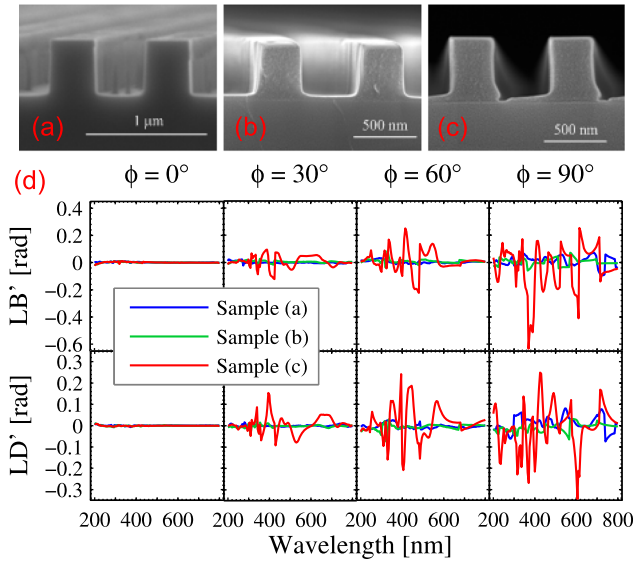

FIG. 4. The spectra of elementary optical properties LB′ and LD′ extracted from the experimental Mueller matrices of samples (a), (b), and (c) collected at different azimuthal angles. In the experiment, the incidence angle was fixed at 65°, and the wavelength was varied from 200 to 800 nm with increments of 5 nm.

fabricated by e-beam lithography followed by dry etching. The nanoimprint process was operated at a temperature of 70 °C with 1 min UV exposure time and 20 min imprint time. The imprint pressure was varied from 10 to 20 bar (1 bar = 10^5 Pa) to make imprinted resist patterns that have different residual layer thicknesses. Figures 4(b) and 4(c) show SEM images of two imprinted gratings with imprint pressures of 20 and 13 bar, respectively. From Fig. 4, we observe that both the Si mold [sample (a)] and the imprinted sample with an imprint pressure of 20 bar [sample (b)] show symmetric profiles (at least with our naked eye), while the imprinted sample with an imprint pressure of 13 bar [sample (c)] obviously does not have a symmetric profile, but exhibits a foot-like asymmetry.

We used an in-house developed Mueller matrix ellipsometer[1] to collect the Mueller matrices of the three samples. Noticeable depolarization effects were observed from the measured data, which were demonstrated to be mainly induced by the finite spectral bandwidth and numerical aperture (NA) of the ellipsometer for samples (a) and (c).[4] The spectral bandwidth and NA of the ellipsometer, which were determined through a measurement on a nominally 1000 nm SiO_2 thick thermal film on the Si substrate, were $\sigma_\lambda = 1.0$ nm and $NA = 0.065$, respectively. Besides these two factors, the nonuniformity of the residual resist layer between the substrate and the imprinted features was demonstrated to also induce depolarization for sample (b).[18] The ±45° linear birefringence and dichroism LB′ and LD′ extracted from the collected Mueller matrix spectra are presented in Fig. 4(d). As expected, the spectra of LB′ and LD′ of sample (c) exhibit much larger variation than those of samples (a) and (b) at the same conical mounting. Moreover, we observe that the spectra of LB′ and LD′ of samples (a) and (b) also show slight differences from zero, especially when $\phi = 90°$, which has been beyond the experimental error (less than 0.01 over most of the spectrum). It indicates that the geometrical profiles of samples (a) and (b) are not completely symmetric, which is reasonable by considering the practical fabrication processes.

IV. CONCLUSIONS

In this work, the Mueller matrix differential decomposition has been applied to understand the use of MME in distinguishing the direction of profile asymmetry. We have found and demonstrated that, among the six elementary optical properties, LB, LD, LB′, LD′, CB, and CD, only the linear birefringence and dichroism along the ±45° axes, LB′ and LD′, exhibit sensitivity to the direction of asymmetric profiles. We have further demonstrated that equal magnitude of profile asymmetry in opposite directions always yields LB′ and LD′ of the same absolute deviation from zero but of opposite sign at any conical mounting. It is worth mentioning that the presented property of LB′ and LD′ is not limited to the detection of the reported asymmetries. It can be extended to any quantities that break structural symmetry, e.g., line edge roughness and overlay errors,[19,20] at many process steps, such as lithography and etch processes.

ACKNOWLEDGMENTS

This work was funded by the National Natural Science Foundation of China (Grant Nos. 51475191, 51405172, 51575214, and 51525502), the Natural Science Foundation of Hubei Province of China (Grant No. 2015CFA005), the China Postdoctoral Science Foundation (Grant Nos. 2014M560607 and 2015T80791), and the Program for Changjiang Scholars and Innovative Research Team in University of China (Grant No. IRT13017).

[1]S. Liu, X. Chen, and C. Zhang, Thin Solid Films **584**, 176 (2015).
[2]J. Li, J. J. Hwu, Y. Liu, S. Rabello, Z. Liu, and J. Hu, J. Micro/Nanolithogr., MEMS, MOEMS **9**, 041305 (2010).
[3]T. Novikova, P. Bulkin, V. Popov, B. H. Ibrahim, and A. De Martino, J. Vac. Sci. Technol., B **29**, 051804 (2011).
[4]X. Chen, C. Zhang, S. Liu, H. Jiang, Z. Ma, and Z. Xu, J. Appl. Phys. **116**, 194305 (2014).
[5]R. M. A. Azzam, J. Opt. Soc. Am. A **68**, 1756 (1978).
[6]R. Ossikovski, Opt. Lett. **36**, 2330 (2011).
[7]N. Ortega-Quijano and J. L. Arce-Diego, Opt. Lett. **36**, 2429 (2011).
[8]J. Schellman and H. P. Jensen, Chem. Rev. **87**, 1359 (1987).
[9]Z. Sekera, J. Opt. Soc. Am. **56**, 1732 (1966).
[10]M. G. Moharam, D. A. Pommet, E. B. Grann, and T. K. Gaylord, J. Opt. Soc. Am. A **12**, 1077 (1995).
[11]C. H. Herzinger, B. Johs, W. A. McGahan, J. A. Woollam, and W. Paulson, J. Appl. Phys. **83**, 3323 (1998).
[12]H. T. Huang, W. Kong, and F. L. Terry, Jr., Appl. Phys. Lett. **78**, 3983 (2001).
[13]H. J. Patrick, T. A. Germer, Y. Ding, H. W. Ro, L. J. Richter, and C. L. Soles, Appl. Phys. Lett. **93**, 233105 (2008).
[14]L. Li, J. Opt. Soc. Am. A **17**, 881 (2000).
[15]W. Ludwig and C. Falter, *Symmetries in Physics: Group Theory Applied to Physical Problems* (Springer, Berlin, 1988).
[16]E. Plum, X.-X. Liu, V. A. Fedotov, Y. Chen, D. P. Tsai, and N. I. Zheludev, Phys. Rev. Lett. **102**, 113902 (2009).
[17]H. C. van de Hulst, *Light Scattering by Small Particles* (Wiley, New York, 1957).
[18]X. Chen, C. Zhang, and S. Liu, Appl. Phys. Lett. **103**, 151605 (2013).
[19]T. Novikova, A. De Martino, R. Ossikovski, and B. Drévillon, Eur. Phys. J.: Appl. Phys. **31**, 63 (2005).
[20]Y.-N. Kim, J.-S. Paek, S. Rabello, S. Lee, J. Hu, Z. Liu, Y. Hao, and W. McGahan, Opt. Express **17**, 21336 (2009).